

Morphotectonics of the Upper Tiber Valley (Northern Apennines, Italy) through quantitative analysis of drainage and landforms

L. Melelli · S. Pucci · L. Saccucci · F. Mirabella ·
F. Pazzaglia · M. Barchi

Received: 22 January 2014 / Accepted: 18 September 2014 / Published online: 9 October 2014
© Accademia Nazionale dei Lincei 2014

Abstract We present a geomorphological analysis of the recent extensional tectonics of a Quaternary continental basin in the Northern Apennines (Italy). The study area is focused on Upper Tiber Valley (UTV), a basin elongated for 70 km in NNW-SSE direction hosting the Tiber River. The area is characterized by a series of features that make it an excellent case study: (i) homogeneity of lithology (ii) active faults, and (iii) strong morphogenetic activity. In this study, 36 hydrographical basins, tributaries of Tiber River, have been analysed. A preliminary qualitative geomorphological setting was outlined pointing out that the drainage river network shows meaningful evidence of tectonic control, such as abrupt changes in stream directions, knickpoints and steepness anomalies alignments along meaningful length in adjacent basins. Besides, the

tectonic control is well marked in base level changes and consequent tectonically induced downcutting. Signs of neotectonics are highlighted by structural landforms too. The entrenchment of alluvial fans, the triangular facets and the fault planes are mapped by field survey and aerial photo interpretation. In addition, a quantitative analysis was also performed. Linear, areal and volumetric indexes related to drainage basins and river networks are taken into account. The geometry of the escarpments delimiting the basin and the landforms detected along the adjacent piedmont are investigated. The ranges of values, according to the existing literature, confirm a condition of wide-ranging morphological disturbance. In the central part of the study area, while the western basins are almost in equilibrium, the eastern ones reveal clear signs of disequilibrium, this is particularly evident along the distal segment of the river network. These data, joined with the characteristics of the escarpment and piedmont junction, confirm that the neotectonic activity, in the centre and in the eastern side of the basin, is the main factor controlling the morphological system.

This peer-reviewed article is part of a coordinated collection of scientific researches on the comparative evolution of intermontane basins of the central-southern Apennines.

L. Melelli (✉) · F. Mirabella · M. Barchi
Dipartimento di Fisica e Geologia, Università di Perugia,
Perugia, Italy
e-mail: laura.melelli@unipg.it

S. Pucci
Istituto Nazionale di Geofisica e Vulcanologia, Rome, Italy

L. Saccucci
Perugia, Italy

F. Mirabella
Istituto di Ricerca per la Protezione Idrogeologica, Consiglio
Nazionale delle Ricerche, via Madonna Alta 126, 06128 Perugia,
Italy

F. Pazzaglia
IntGeoMod s.r.l., Via Innamorati 7/a, 06123 Perugia, Italy

Keywords Geomorphometry · Neotectonic ·
Tiber basin · Umbria region

1 Introduction

The extensional intermountain basins of central Italy are the key areas for tectonic geomorphology and landscape observation resulting from the interaction between crustal (both vertical and horizontal) deformation and surface modelling processes (Schiattarella et al. 2003; Sagri et al. 2004; Bull 2008; Bartolini 2012). From a morphological point of view, the basins are flat areas sharply separated by

a relief in correspondence with a fault plane often masked by debris, colluvial or alluvial deposits. In particular, the mountain piedmont junction is the area where the morphological evidences of the competition between regional uplift, faults activity and erosional/deposition processes are emphasized. The derived landforms can be investigated in order to define geomorphical indexes useful for a tectonic classification of the mountain fronts (hereinafter referred to as MF; Bull 2008).

In the inner and axial segments of the Northern Apennines, a large number of extensional tectonic basins, with such morphological characteristics, are present. These basins were formed during the extensional activity started in the upper Pliocene, and are still active along the axial culmination of the Northern Apennines. They vary from 10 to 40 km in length and between few kilometres up to 20 km in width, with areal extent decreasing towards the east. Moreover, they are characterized by syn-tectonic sedimentation, represented by both shallow marine and fluvial–lacustrine deposits, with a maximum thickness up to 3.0 km (Sagri et al. 2004). The graben or semi-graben structure requires that at least one of the slopes bordering the basin is coincident with a recent fault plane or with a fault-line scarp and that the other side is corresponding to an antithetic fault.

In this contribution, new geological and geomorphological data of the Upper Tiber Valley (UTV) in the Northern Apennines are presented. The UTV is the northern part of the Tiber Basin (Umbria, Central Italy) extending on an area of about 1,800 km² from Sansepolcro to Perugia where it diverges in two branches reaching the southern limit of the region (Basilici 1997). The existing literature on the area is particularly focused on the tectonic genesis of the basin (Barchi et al. 1991; Barchi and Ciaccio 2009) in relationship with the action of the Alto Tiberina Fault (ATF), a low-angle ($\sim 20^\circ$) normal fault with a NNW-trend that accumulated over about 10 km of horizontal displacement during the last 3 Ma (Collettini and Barchi 2002; Delle Donne et al. 2007; Mirabella et al. 2011). The stratigraphical and sedimentological characteristics of the basin infill are described in a few works where the Pliocene–Pleistocene deposits are classified, correlated and dated (Conti and Girotti 1977; Ambrosetti et al. 1987; Basilici 1997; Pucci et al. 2014).

Recent research has been focused on a multidisciplinary approach in order to evaluate the morphotectonic evolution of the entire valley (Mirabella et al. 2010; Meelli et al. 2012; Pucci et al. 2014). In this paper, a qualitative geomorphological analysis, performed on the entire study area is reported, while a quantitative analysis was addressed to the central part of the study area. Different geomorphical indexes have been also calculated in order to highlight the difference between the west and east sides of the valley and

better understand the specific relationship between the regional uplift and the local subsidence and the role of the fault systems in the development of the valley.

2 Methods

The mountain fronts (MFs) can be divided into different components, both morphological and hydrographical. The investigation of each of these components is performed using two main approaches: a qualitative method including field survey, aerial-photo interpretation and mapping analysis and a quantitative one, in order to obtain numerical indexes (Belisario et al. 1999; Lupia Palmieri et al. 2001; Ciotoli et al. 2003; Beneduce et al. 2004; Troiani and Della Seta 2011). The morphometric indexes are extracted from a digital elevation model (DEM) with a cell size of 90×90 m. The DEM derives from the Shuttle Radar Topography Mission (SRTM) providing a high vertical accuracy, in particular in the flat areas, near the connection with the Tiber river.

2.1 Mountain piedmont junction and adjacent piedmont landforms

The geometry of the contact between steep slopes bounding a basin and the plain area (i.e. mountain piedmont junction) is measurable by the mountain front sinuosity index (S_{mf}). This index quantifies the morpho-evolution rate of a fault plane and is equal to the ratio of the curvilinear length along the piedmont junction and the straight distance between the endpoints of its MF (Bull and McFadden 1977). Sinuosity is directly proportional to the time formation of fault plane and bedrock erodibility. S_{mf} less than 1.4 indicates tectonically active fronts (Keller 1986), whereas values greater than 3 are typical for inactive MF (Bull and McFadden 1977). Entrenched alluvial fans are adjacent piedmont landforms related to the ratio of sedimentation and uplift rate, and can be translated in different tectonic activity classes (Bull 2008).

2.2 Escarpment

Active extensional basins are bordered by rectilinear steep escarpment to relative uplift of the normal faults footwall, showing structural landforms as aligned triangular facets. The comparisons of number, areal extension and preservation of triangular facets are a function of neotectonic activity (Bull 2008). The lithological characteristics being equal and the weathering homogeneous, the differences in triangular facets preservation are related to dissimilarities in tectonic exhumation rates.

2.3 River network and drainage basins

The qualitative observation comprises the identification of irregular pattern of watercourses, in particular in proximity of the confluences and along the threshold areas of the basins. The differences in areal extent of alluvial deposits are also considered. The main purpose is to highlight the anomalies and investigate the mutual spatial distribution of the related landforms. By modelling the rivers in a one-dimensional network, a hierarchization (Horton 1945; Strahler 1980) verifies the bifurcation ratio R_b , equal to the ratio of the number of streams of any order to the number of streams of the next highest order, ideally equal 2. R_b values range between 3 and 5 (Goudie 2004). The analysis of the longitudinal profile is the second step. In general, a river typically shows a smoothly concave-upward geometry. The shape of the curve is well described by the Flint's law (Flint 1974) $S = k_s A^{-\theta}$, where S is the channel local slope, k_s is the steepness index, A is the contributing area (m^2) and θ is the concavity index. This equation is valid for each point of the basin and is usually represented in a bi-logarithmic plot. The steepness index, equal to the intercept of the regression line, is directly connected to the uplift rate and to climate and lithology. A graded stream is characterized by k_s values decreasing towards the base level. The concavity, equal to the slope of the regression line, varies between 0 and 1, with most values typically clustering between 0.4 and 0.6. It is not related to tectonic uplift, but a strong variation in basin lithology can affect the values (Tucker and Whipple 2002). The Stream Profiler tool for ArcGIS 9.x © ESRI (Whipple et al. 2007) was used in order to extract the indexes. A plot is computed to highlight the observed and predicted channel profiles, and the knickpoints' positions are identified. Then, different k_s values along the profile can be detected with the related θ value. A medium concavity index for the profile is also computed (Wobus et al. 2006). When imported in ArcGIS, the k_s values are plotted along the rivers, which, for each basin, are classified into five classes. The break values are selected with the Jenk's algorithm.

The Drainage density (D_d), defined as the cumulative length of all stream channels in a drainage basin, divided by the drainage basin area (Horton 1945), provides an estimate of the permeability of the substrate and assures the necessary uniformity in lithological conditions. The watershed or basin shape is quantified by the circularity factor (R_c) which is defined as the ratio between the surface area of the drainage basin and the surface of the circle having the perimeter equal to the length of the line of the watershed basin which is considered. The structural conditions, both passive and active factors, prevail in elongated basins with low values of R_c . Finally, the relief

aspect, defined as the percentage hypsometric curve (Strahler 1980), quantifies the landmass distribution from the top to the base of the drainage basins and is represented by a function ranging from 0 to 1. Since it is scale-independent, it is particularly useful to compare drainage basins with different dimensions. The hypsometric curves are computed by the SRTM DEM in a GIS both for the values of area and altitude.

3 The Upper Tiber valley: geological setting

The Upper Tiber Valley (UTV, Figs. 1, 2, 3) is the northern part of the larger Tiberino Basin (Lotti 1926), in the Northern Apennines (central Italy). Since Late Pliocene, an extensional tectonic phase has affected the area. Since the Middle Pleistocene, and still active, an isostatic uplift, of the order of 0.5–1 mm/year, also occurred (Ambrosetti et al. 1982; D'Agostino et al. 2001). The study area is located at the hanging wall of the AltoTiberina normal Fault. The substratum cropping out in the mountain area is quite homogeneous with the prevalence of Umbrian silicoclastic units and, in a narrow south-western portion of the Umbria-Marche carbonate multilayer (Perugini Mountains). The Tiber river basin is infilled with a thick fluvial-lacustrine sequence. From bottom to the top, the following units are present: the Fighille Unit (Early Pleistocene), with prevalent grey clay; the Citerma Unit (Early Pleistocene), with sands and gravels of braided fluvial environment; and the Promano Unit (Upper Early Pleistocene), with sands of fluvial environment. The Valliano Unit (Middle Pleistocene) at the top, is formed by monogenic conglomerates (proximal alluvial fan deposits). All units are heterogeneous in thickness and laterally discontinuous (Pucci et al. 2014).

4 Data analysis

4.1 Qualitative geomorphological assessment

Within the UTV, some geomorphological features allow us to recognize three sub-basins (Pucci et al. 2014). From north to south: the Sansepolcro, Umbertide and Ponte Pattoli sub-basins. Thresholds between the sub-basins are identified by abrupt narrowing of the valley width and tilting of Pleistocene deposits, a meandering pattern of the Tiber river and well-defined deviations according to discontinuities transversal to the basin.

The Sansepolcro sub-basin (Fig. 1) is the largest one (width of up to 4,500 m), and it is totally covered by the Tiber river alluvial deposits. The eastern boundary is characterized by the absence of Pleistocene deposits and by

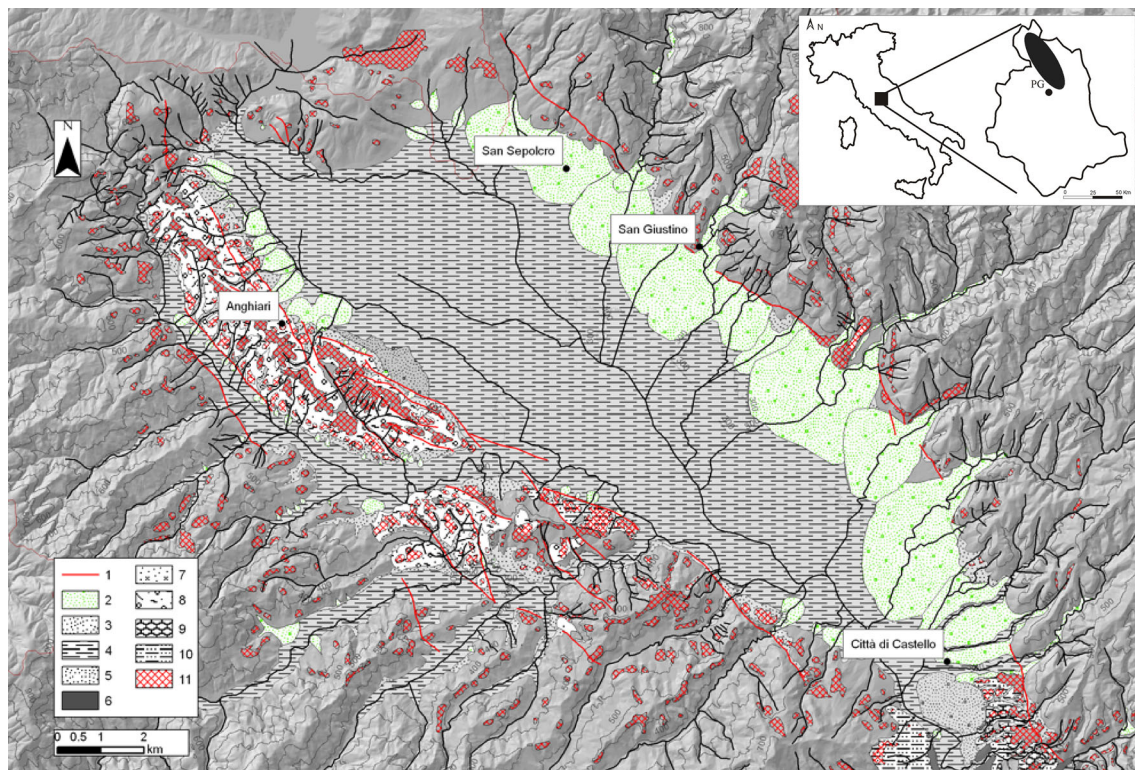


Fig. 1 The Sansepolcro sub-basin 1 faults, 2 alluvial fans, 3 colluvial deposits, 4 alluvial deposits, 5 fluvial terraces (II order), 6 fluvial terraces (I order), 7 Promano unit, 8 Citerna unit, 9 Valliano unit, 10 Fighille unit, 11 paleosurfaces. In the *upper right*, the location map of the study area

large triangular facets. A continuous bajada of alluvial fan zone is present, the largest of the entire UTV. In the southern portion of the sub-basin, near the threshold, the alluvial fans are deeply entrenched. The rivers are perpendicular to the basin and characterized by a strong erosional activity. A NW–SE trending fault system controls the western side, tilting the river terraces as the result of the east-dipping faults (Cattuto et al. 1995) that were active between the Middle Pleistocene and the Holocene, with an offset of about 190 m (Delle Donne et al. 2007). The rivers display evidence of sedimentation with large alluvial fans.

Within the Umbertide sub-basin (Fig. 2), a unique order of fluvial terrace is present on the western boundary, while on the opposite side two orders are detectable. In both cases, the landforms are classified as strath terraces with thin alluvial deposit covering a substratum consisting of the Fighille and Citerna units. The top of the terraces near Città di Castello has a 15° north dip direction (Pucci et al. 2014). The alluvial deposits are downcut by the drainage network, and so fluvial erosion prevails on tectonic uplift. Along the eastern boundary, an abrupt junction, marked by slope breaks and counterslopes alignments, connects the pre-Pliocene bedrock and a hilly area made of the Pleistocene deposits. The rivers show a parallel pattern with a flow direction perpendicular to the development of the valley

and headward erosion, suggesting a continuous base level lowering. The alluvial fans are almost absent.

Within the Ponte Pattoli sub-basin (Fig. 3), the Tiber river presents a talweg always leaning against the western boundary, defining an asymmetrical valley. Two orders of river terraces are present along the eastern limit of the basin with a minor difference (20 m) between the two treads and between the tread of the second order and the alluvial plain with respect to the Umbertide segment. On the western boundary, the terraces are absent. The eastern rivers have a parallel pattern and show a strong tendency to the headward erosion. The distinctive character of this sub-basin is the almost total absence of Pleistocene deposits on the right bank, where the bedrock abruptly comes into contact with the floodplain through a series of aligned triangular facets.

4.2 Quantitative measurement of landscape

The UTV is a very suitable test area for geomorphical analysis because it allows highlighting different responses of morphological system to tectonic impulses. The bedrock is homogeneous, as confirmed by similar drainage density (D_d) and bifurcation ratio (R_b) values (Tables 1, 2). 36 basins are present: 22 on the eastern side of the basin and

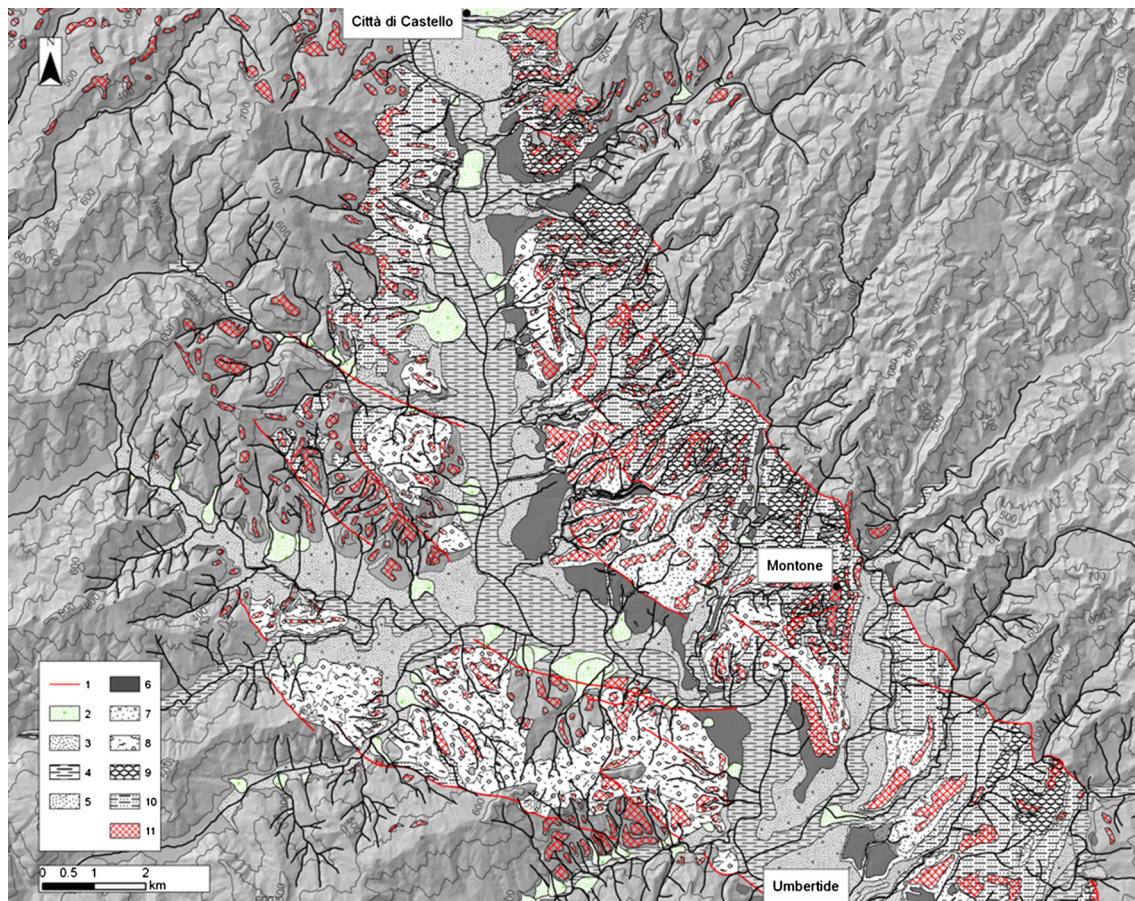


Fig. 2 The Umbertide sub-basin 1 faults, 2 alluvial fans, 3 colluvial deposits, 4 alluvial deposits, 5 fluvial terraces (II order), 6 fluvial terraces (I order), 7 Promano unit, 8 Citerna unit, 9 Valliano unit, 10 Fighille unit, 11 paleosurfaces

14 on the western one (Fig. 4). The triangular facets are well recognizable in the eastern limit of Sansepolcro and in the western limit of Ponte Pattoli sub-basins. In the first case, the facets show erosional landforms with valleys extending more than 0.7 of the ratio between the distance along the horizontal direction and the base and the top of the facet (class 3, Bull 2008). Within the Ponte Pattoli basin the planar surfaces show shallow valleys extending on a short distance on the facet (class 2, Table 1, Bull 2008). The largest and entrenched fans occur in the upper part (with a mean area of 6 km²) and are located along the eastern side of Sansepolcro sub-basin. The other fans are smaller (average area ca. 0.09 km²) and are distributed on the western side of Sansepolcro and Umbertide sub-basin (Fig. 4). In order to estimate the S_{mf} values, the mountain piedmont junction is divided into nine segments along the contact between the bedrock and the alluvial deposits (Fig. 4). The western side of Sansepolcro sub-basin is the only portion of the study area that is not taken into account. On this boundary the Quaternary deposits are faulted and uplifted in a gentle hill and the limit between the bedrock and the bottom of the basin is not along a unique well-

defined escarpment as in the rest of the UTV. The mountain fronts n. 1, 5 and 7 have S_{mf} values <1.4. The lowest values of S_{mf} (1.3) are distributed on the eastern side of the Sansepolcro sub-basin and on the southwestern boundary of Umbertide one. The other values are referred to a non-tectonically active MF (Fig. 4).

The analysis on the drainage network was focused only on the Umbertide sub-basin. Within the Sansepolcro one the qualitative evidences and the previous knowledge outline a prevalent sedimentation. The Ponte Pattoli area shows a strong difference in bedrock composition between the eastern silicoclastic units and the western limestones. Accordingly, the area is not adequate to test the morphometric indexes. A quantitative comparison between the two sides of the valley might confirm the evolutionary model emerging from the background studies and qualitative observations. To test this possibility, five basins are taken into account: the eastern ones are n. 10, 13 and 15 (Soara, Carpina and Assino); the western n. 31 and 32 (Niccone and Nestore). The hypsometric curves of the western basins underline an evident concavity connected to a uniform erosional activity needed to achieve a stadium of

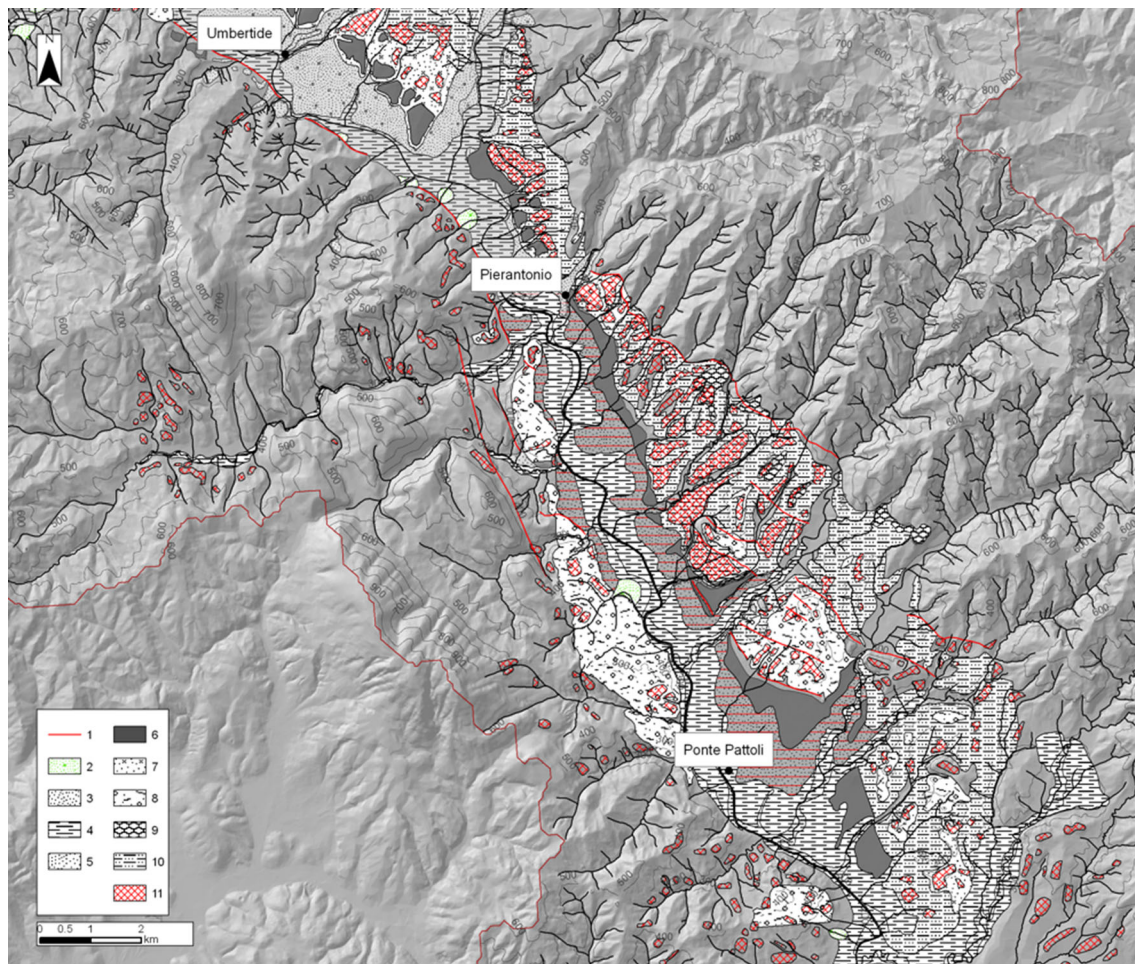


Fig. 3 The Ponte Pattoli sub-basin 1 faults, 2 alluvial fans, 3 colluvial deposits, 4 alluvial deposits, 5 fluvial terraces (II order), 6 fluvial terraces (I order), 7 Promano unit, 8 Citerna unit, 9 Valliano unit, 10 Fighille unit, 11 paleosurfaces

equilibrium (Fig. 5a). The eastern ones highlight convex curves, where stream erosion is the most meaningful denudation process (Fig. 5b). Moreover, the final segment points out an inflection in the final part of the line, as further evidence that a renewal of the erosional activity is acting. The position is not coincident with the transition between bedrock and Pleistocene deposits but always remains inside the latter. The concavity index ranges between 0.31 and 0.41, near the reference value of 0.5 (Fig. 6). The steepness index decreases regularly from the top to the bottom of the basin in the western portion of the area, the highest values corresponding to the headwater areas. So, the index underlines a substantial equilibrium along the river network growth (Fig. 6). The eastern basins reflect the behaviour of the entire left side of the UTV with smaller and, on average, narrow and elongated catchments (Table 2). The steepness index (Fig. 6) shows an anomalous trend with a sudden increase in the lowest part of the catchments. The highest values of steepness index are aligned along the three catchments taken into account.

5 Discussion and conclusion

We define a quantitative geomorphological analysis to identify and analyse cross-sectional and longitudinal discontinuities within the Upper Tiber Valley, due to tectonic and structural factors.

Although today the three sub-basins form a unique geographical and morphological unit, due to the Tiber river connection, from a morphotectonic point of view, the Sansepolcro sub-basin is totally different in the geomorphological evolution. The thresholds separating the three sub-basins are the morphological evidences of transfer zones caused by the different behaviours of the hanging wall blocks.

The Sansepolcro basin is deep and filled with tens of meters of Holocene alluvial deposits, with poor exhumation of Pleistocene deposits. Alluvial deposits without fluvial terraces are present. The basin shape is the widest of the study area, with evidence of faulting both on the western and on the eastern limits. In particular, the latter is

Table 1 Morphometric indexes for the eastern tributaries of river Tiber

| No | River | Area (km ²) | Perimeter (km) | K_{\max} | R_b | D_d | R_c |
|----|---------------|-------------------------|----------------|------------|-------|-------|-------|
| 1 | Afra | 35.83 | 43.74 | 3 | 5.3 | 1.10 | 0.24 |
| 2 | Vertola | 16.82 | 27.43 | 3 | 3.8 | 0.90 | 0.28 |
| 3 | Valecchio | 7.91 | 15.56 | 3 | 2.8 | 1.80 | 0.41 |
| 4 | Selci | 43.73 | 44.82 | 4 | 4.0 | 1.40 | 0.27 |
| 5 | Piosina | 8.34 | 16.90 | 3 | 2.9 | 2.00 | 0.37 |
| 6 | Regnano | 23.25 | 40.68 | 4 | 3.1 | 1.00 | 0.18 |
| 7 | Vaschi | 22.40 | 33.04 | 4 | 3.2 | 1.10 | 0.26 |
| 8 | Basin 8 | 11.26 | 15.99 | 3 | 3.2 | 0.00 | 0.55 |
| 9 | Scatorbia | 13.45 | 22.22 | 3 | 3.2 | 1.40 | 0.34 |
| 10 | Soara | 64.39 | 54.54 | 4 | 4.3 | 1.60 | 0.27 |
| 11 | Rancale | 18.02 | 21.41 | 4 | 2.9 | 1.70 | 0.49 |
| 12 | Lana | 28.90 | 38.88 | 3 | 5.2 | 1.40 | 0.24 |
| 13 | Carpina | 130.94 | 85.14 | 5 | 3.5 | 1.20 | 0.23 |
| 14 | Reggia | 12.75 | 21.59 | 3 | 3.3 | 1.00 | 0.34 |
| 15 | Assino | 174.17 | 86.22 | 5 | 3.8 | 1.40 | 0.29 |
| 16 | Mussino | 20.61 | 32.04 | 3 | 4.9 | 1.50 | 0.25 |
| 17 | Parlesca | 15.56 | 21.67 | 3 | 3.3 | 1.50 | 0.42 |
| 18 | S. Bartolomeo | 5.42 | 12.53 | 3 | 2.5 | 1.90 | 0.43 |
| 19 | Resina | 28.17 | 41.04 | 4 | 3.6 | 1.50 | 0.21 |
| 20 | Ventia | 48.10 | 50.04 | 4 | 3.9 | 1.20 | 0.24 |
| 21 | Rio Grande | 28.50 | 41.40 | 3 | 4.9 | 1.10 | 0.21 |
| 22 | Il Rio2 | 24.73 | 42.84 | 4 | 2.8 | 1.50 | 0.17 |

Table 2 Morphometric indexes for the western tributaries of river Tiber

| No | River | Area (km ²) | Perimeter (km) | K_{\max} | R_b | D_d | R_c |
|----|-----------|-------------------------|----------------|------------|-------|-------|-------|
| 23 | Il Rio | 18.45 | 20.64 | 3 | 4.6 | 1.30 | 0.54 |
| 24 | Giordana | 4.46 | 9.70 | 3 | 3.3 | 1.50 | 0.60 |
| 25 | Montenero | 6.93 | 11.72 | 3 | 3.5 | 1.40 | 0.63 |
| 26 | Molinella | 9.13 | 14.97 | 3 | 3.8 | 1.80 | 0.51 |
| 27 | Bruna | 9.70 | 16.69 | 3 | 3.5 | 1.50 | 0.44 |
| 28 | Nese | 41.38 | 45.18 | 4 | 5.0 | 1.60 | 0.25 |
| 29 | Badia | 6.34 | 12.73 | 3 | 3.8 | 1.50 | 0.49 |
| 30 | Tonne | 5.57 | 14.25 | 3 | 2.5 | 1.50 | 0.34 |
| 31 | Niccone | 151.28 | 75.42 | 5 | 3.5 | 1.50 | 0.33 |
| 32 | Nestore | 212.24 | 86.04 | 5 | 4.2 | 1.30 | 0.36 |
| 33 | Aggia | 43.11 | 53.46 | 4 | 4.0 | 1.00 | 0.19 |
| 34 | Erchi | 14.94 | 24.58 | 2 | 3.5 | 0.45 | 0.31 |
| 35 | Scarzola | 19.13 | 28.95 | 3 | 3.7 | 0.60 | 0.29 |
| 36 | Cerfone | 265.00 | 103.35 | 5 | 4.6 | 1.30 | 0.31 |

an indication for a tectonically active MF with an abrupt contact. The plain is masked by coalescent alluvial fans and triangular facets aligned along the escarpment. The S_{mf}

index is also typical of tectonically active MF. The alluvial fans are entrenched, testifying to a key role played by stream-channel downcutting (Bull 2008).

The Umbertide and Ponte Pattoli sub-basins are characterized by thin (less than ten meters) Holocene alluvial deposition and by incision of the Quaternary sedimentary units. The Tiber erosion prevails allowing the emplacement of two orders of fluvial terraces. The basin's extent decreases with the main direction of the basin axes, which changes abruptly from the north–south to the NW–SE. The S_{mf} index has a wide spectrum of values. Only the segments on the western margin of the basin can be attributed to tectonically active MF; a few, not continuous and very small alluvial fans, are present.

The drainage network shows significant differences between the eastern and western flanks of the Tiber Valley. On the eastern side, the shape of basins is almost everywhere elongated. Moreover, the steepness and the concavity indexes, estimated on the Umbertide sub-basins, show a clear increase of the steepness along a well-defined zone which is longitudinally continuous and has the same direction of the main splays system. The hypsometric curves also show the same anomalous behaviour. This reflects a condition of minor equilibrium for the eastern drainage network.

Two different evolutionary models for the separation of the Sansepolcro from Umbertide and Ponte Pattoli basins, based on different rates of regional uplift vs. local subsidence, can be proposed.

In the Sansepolcro sub-basin, the activity of normal faults resulted in a strong subsidence: maximum subsidence is detected in the centre of the sub-basin and is higher than the regional uplift rate. On the eastern edge of the valley, the thickness of the alluvial fan deposits decreases towards Città di Castello, where the fans are more entrenched. Within this sub-basin, the activity of antithetic faults seems to be predominant. The eastern-bounding fault, antithetic to the ATF, follows the style and the direction of the master faults delimiting the Gubbio basin, to the east of the study area, where the main antithetic splay of ATF is present. According to MF classification, and considering the results of qualitative and quantitative analyses, this limit is tectonically active.

Within the Umbertide and Ponte Pattoli sub-basins, the evolutionary model highlights that the regional uplift is greater than subsidence induced by fault systems bordering the basin. The location of active tectonic elements, according to the morphometric indexes, places the active mountain fronts along the western edge of the valley, where the synthetic splays are present. The Tiber river flows against the western slopes. In contrast, the greater evidence of drainage network disequilibrium is focused in the eastern watersheds, delimited by the ATF antithetic splays. The splays are localized both on the contact between bedrock

Fig. 4 Drainage basins and river network of river Tiber tributaries. The numbering of basins is referred to Tables 1, 2. From 1 to 5, Horton–Strahler ordering of hierarchical networks, 6 Tiber river, 7 mountain front labelled with sinuosity index values, 8 alluvial deposits, 9 alluvial fans, 10 Pleistocene deposits

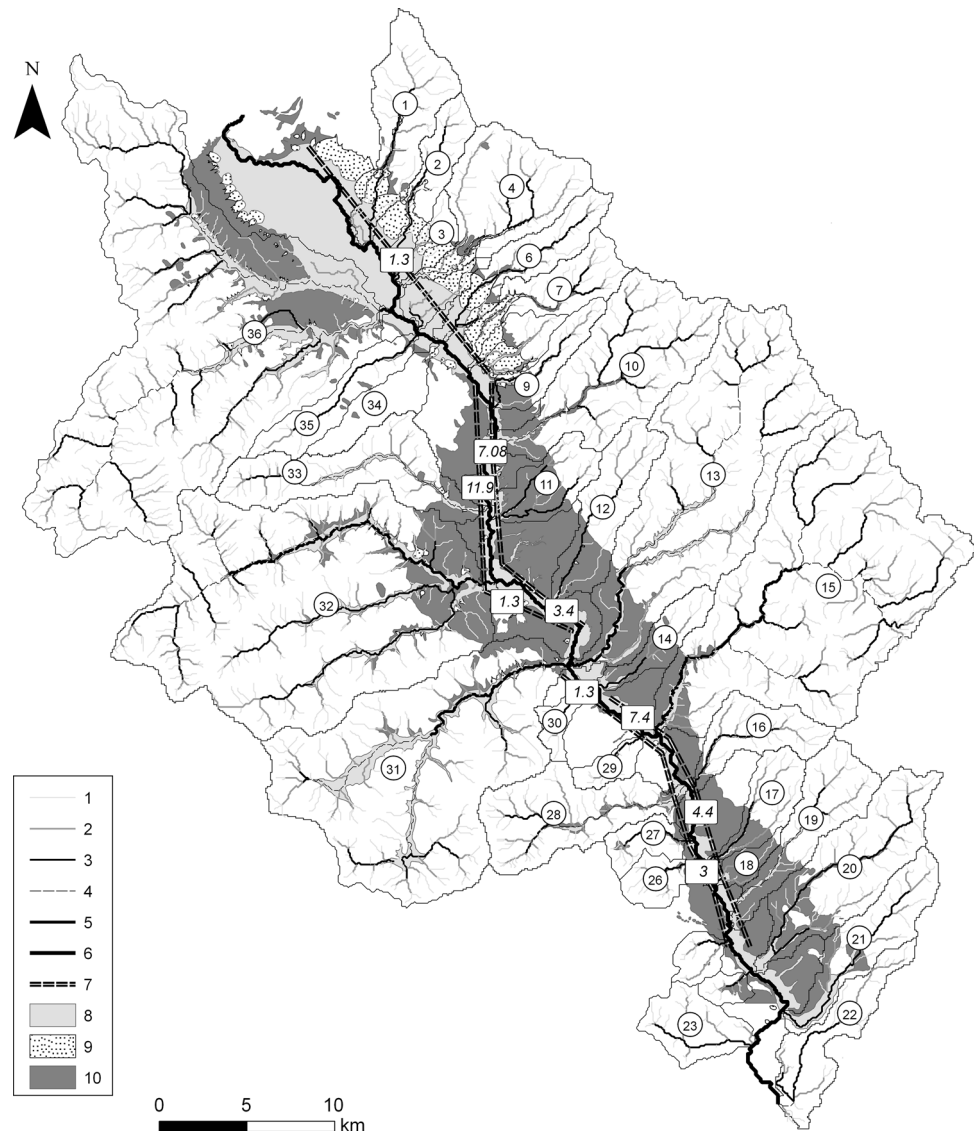


Fig. 5 Hypsometric curves of the Umbertide sub-basins **a** western basins, **b** eastern basins with convex curves highlighting strong erosion

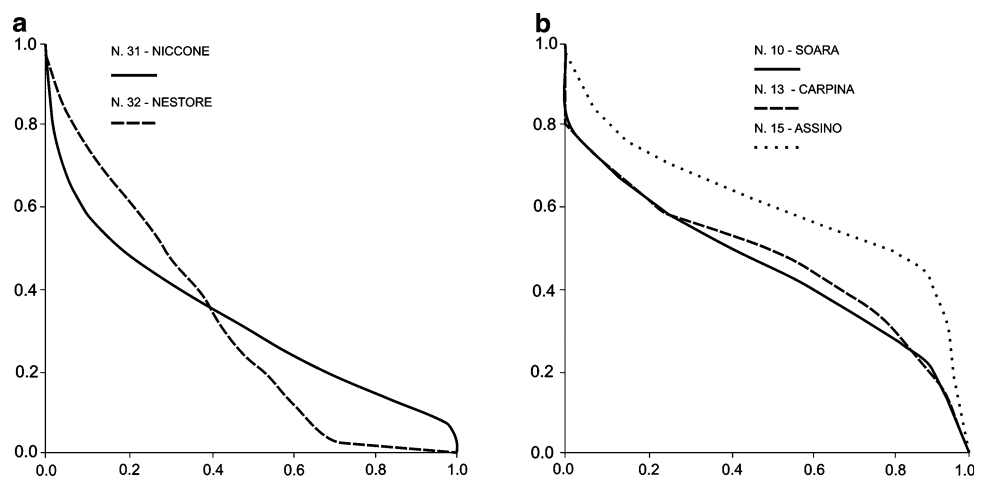


Fig. 6 Steepness index increasing from 1 to 5. The original values are classified, for each basin, according to Jenks natural breaks

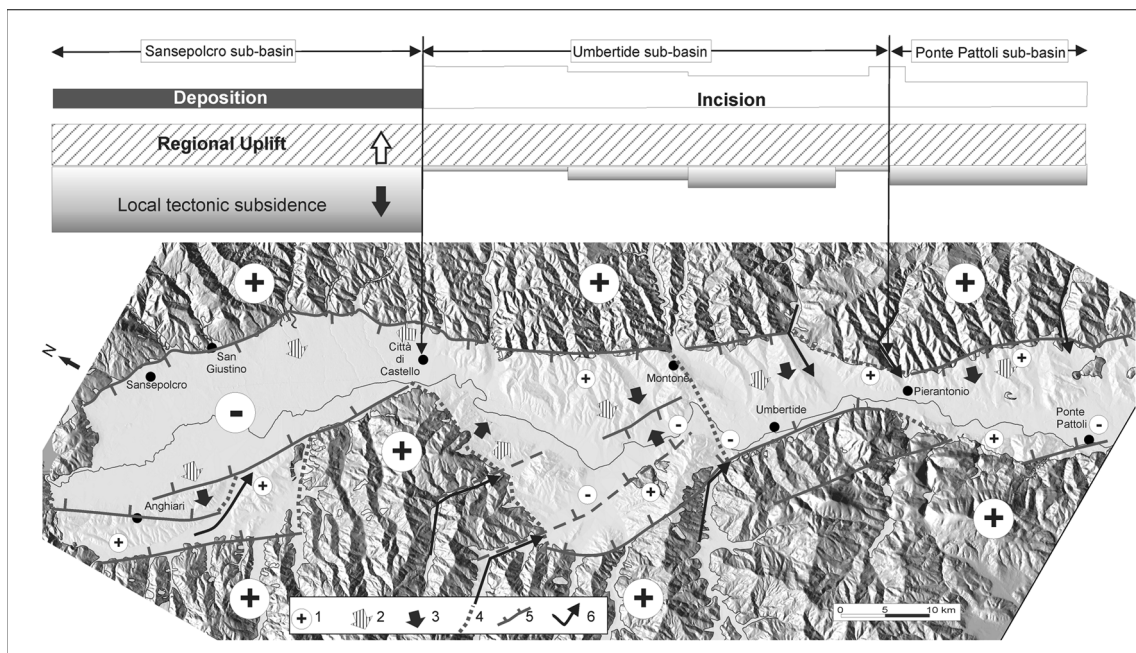
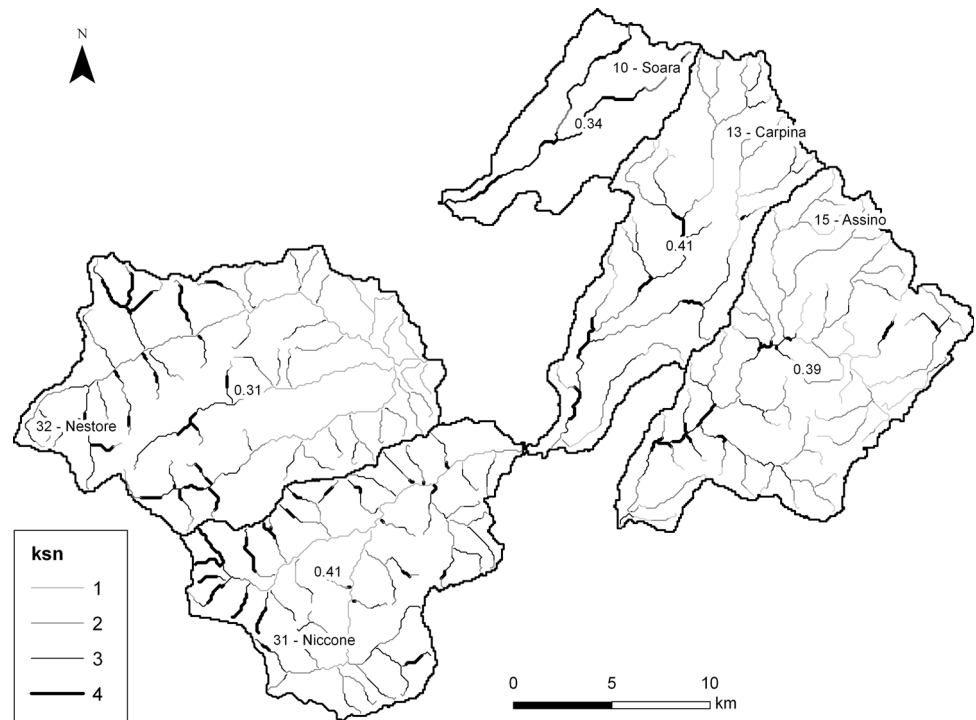


Fig. 7 Evolutionary scheme of UTV 1 uplift (+) or subsidence (-) areas, 2 morphological surfaces dipping direction, 3 tectonic surfaces dipping direction, 4 transfer zones, 5 faults, 6 anomalies in river direction (modified from Pucci et al. 2014)

and Pleistocene deposits and inside the deposits, as highlighted by the longitudinal profiles and by the alignment of the structural landforms. In particular, the Umbertide sub-basin is bordered by the Nestore fault, causing the greater subsidence of the central–southern part of the sub-basin. Within the Ponte Pattoli sub-basin, the west-dipping faults, recognized at the base of Perugini Mountains, lead to the

higher subsidence of the central–southern part of the sub-basin, where the alluvial plain is tilted towards SW.

The disequilibrium of the eastern basins is due to an uplift of the corresponding bedrock. Two different interpretative models chosen can explain this uplift, both based on a low-angle east-dipping fault or on a west-dipping, high-angle fault. In both the models, the eastern block is

uplifted compared with the initial stage. The chosen interpretative model considers an east-dipping fault system, as highlighted by the asymmetry of the valley and of the MF classification (Fig. 7).

The coexistence of the two such different evolutionary models (Sansepolcro and Umbertide–Ponte Pattoli sub-basins) within the study area is due to different subsidence rates compared with a homogeneous regional uplift, equal to about 0.5 mm/y (D’Agostino et al. 2001).

References

- Ambrosetti P, Carraro F, Deiana G, Dramis F (1982) Il sollevamento dell’Italia centrale tra il Pleistocene inferiore e il Pleistocene medio. Contributo conclusivo per la realizzazione della Carta Neotettonica d’Italia (II), CNR Progetto Finalizzato “Geodinamica, S.P. Neotettonica”, 356, pp 1341–1343
- Ambrosetti P, Carboni MG, Conti MA, Esu D, Girotti O, La Monica GB, Landini B, Parisi G (1987) Il Pliocene ed il Pleistocene del Bacino del fiume Tevere nell’Umbria Meridionale. *Geogr Fis Dinam Quat* 10:10–33
- Barchi MR, Ciaccio MG (2009) Seismic images of an extensional basin, generated at the hanging wall of a low-angle normal fault: the case of the Sansepolcro basin (central Italy). *Tectonophysics* 479:285–293
- Barchi M, Brozzetti F, Lavecchia G (1991) Analisi strutturale e geometrica dei bacini della media Valle del Tevere e della Valle Umbra. *Boll Soc Geol It* 110
- Bartolini C (2012) Is the morphogenetic role of tectonics overemphasized at times? *Bollettino di Geofisica Teorica e Applicata* 53(4):459–470
- Basilici G (1997) Sedimentary facies in an extensional and deep-lacustrine depositional system: the Pliocene Tiberino basin, central Italy. *Sediment Geol* 109:73–94
- Belisario F, Del Monte M, Fredi P, Funicello R, Lupia Palmieri E, Salvini F (1999) Azimuthal analysis of stream orientations to define regional tectonic lines. Fourth International Geomorphology Conference, Bologna. *Zeitschrift fur Geomorphologie, Suppl-Bd* 118, pp 41–63
- Beneduce P, Festa V, Francioso R, Schiattarella M, Tropeano M (2004) Conflicting drainage patterns in the Matera Horst Area southern Italy. *Phys chem Earth* 29:717–724
- Bull WB (2008) Tectonic geomorphology of mountains: a new approach to paleoseismology. Blackwell, p 316. ISBN-13: 978-1405154796
- Bull WB, McFadden L (1977) Tectonic geomorphology north and south of the Garlock fault, California. In: Doehring DO (ed) *Geomorphology in arid regions publications in geomorphology*. State University of New York, Binghamton, pp 115–138
- Cattuto C, Cencetti C, Fisauli M, Gregori L (1995) I bacini pleistocenici di Anghiari e Sansepolcro nell’alta valle del F. Tevere *Il Quaternario* 8(1):119–128
- Ciotoli G, Della Seta M, Del Monte M, Fredi P, Lombardi S, Lupia Palmieri E, Pugliese F (2003) Morphological and geochemical evidence of neotectonics in the volcanic area of Monti Vulsini (Latium, Italy). *Quatern Int* 101–102(2003):103–113
- Colletini C, Barchi MR (2002) A low-angle normal fault in the Umbria region (central Italy): a mechanical model for the related microseismicity. *Tectonophysics* 359:97–115
- Conti MA, Girotti O (1977) Villafranchiano del “Lago Tiberino”: ramo sud occidentale, schema stratigrafico e tettonico. *Geol Romana* 16:67–80
- D’Agostino N, Jackson J, Dramis F, Funicello R (2001) Interaction between mantle upwelling, drainage evolution and active normal faulting: an example from the central Apennines (Italy). *Geophys J Int* 147:475–497
- Delle Donne D, Piccardo L, Odum JK, Stephenson WJ, Williams RA (2007) High-resolution shallow reflection seismic image and surface evidence of the Upper Tiber Basin active faults (Northern Apennines, Italy). *Boll Soc Geol Ital* 126(2):323–331
- Flint JJ (1974) Stream gradient as a function of order, magnitude, and discharge. *Water Resour Res* 10(5):969–973
- Goudie A (2004) *Encyclopedia of geomorphology Vol 2*. Taylor and Francis Group Ed, Beijing
- Horton RE (1945) Erosional development of stream and their drainage basins: hydrophysical approach to quantitative morphology. *Geol Soc Am Bull* 56:275–370
- Keller EA (1986) Investigation of active tectonics: use of surficial earth processes. In: Wallace RE (ed) *Active tectonics studies in Geophysics*. National Academies Press, Washington, DC, pp 136–147
- Lotti B (1926) Descrizione geologica dell’Umbria. *Memorie Descrittive della Carta Geologica d’Italia*, 21, p 320
- Lupia Palmieri E, Centamore E, Ciccacci S, D’Alessandro L, Del Monte M, Fredi P, Pugliese F (2001) Geomorfologia quantitativa e morfodinamica del territorio abruzzese III–II bacino idrografico del Fiume Saline. *Geogr Fis Dinam Quat* 24(2):157–176
- Melelli L, Saccucci L, Fiorucci L, Barchi M, Mirabella F, Pazzaglia F, Pucci S (2012) Geomorphological quantitative analysis of high Tiber Valley drainage network (Umbria, Italy). *Rend Online Soc Geol It* 21, parte II, 1120–1121
- Mirabella F, Barchi M, Brozzetti F, Lupattelli A, Melelli L, Saccucci L, Pazzaglia F, Pucci S. (2010) Morphotectonic evolution of a quaternary basin driven by a segmented low-angle extensional system. *Rendiconti Online della Società Geologica Italiana*
- Mirabella F, Brozzetti F, Lupattelli A, Barchi MR (2011) Tectonic evolution of a low-angle extensional fault system from restored cross-sections in the Northern Apennines (Italy). *Tectonics*, 30, TC6002, doi:10.1029/2011TC002890
- Pucci S, Mirabella F, Pazzaglia F, Barchi MR, Melelli L, Tuccimei P, Soligo M, Saccucci L (2014) Interaction between regional and local tectonic forcing along a complex quaternary extensional basin: Upper Tiber Valley, Northern Apennines, Italy. *Quat Sci Rev* 102:111–132. doi:10.1016/j.quascirev.2014.08.009
- Sagri M, Martini IP, Pascucci V (2004) Sedimentary and tectonic evolution of selected neogene–quaternary basins of the Apennines (Italy). Field trip guide books. 32nd International Geological Congress, Florence–Italy, 20–28 August 2004. 4, pp 14–36
- Schiattarella M, Di Leo P, Beneduce P, Giano SI (2003) Quaternary uplift vs tectonic loading: a case-study from the Lucanian Apennine, southern Italy. *Quatern Int* 101–102:239–251
- Strahler AN (1980) System theory in general geography. *Phys Geogr* 1:1–27
- Troiani F, Della Seta M (2011) Geomorphological response of fluvial and coastal terraces to quaternary tectonics and climate as revealed by geostatistical topographic analysis. *Earth Surf Proc Land* 36(9):1193–1208. doi:10.1002/esp.2145
- Tucker GE, Whipple KX (2002) Topographic outcomes predicted by stream erosion models: sensitivity analysis and intermodal comparison. *J Geophys Res* 107(B9):2179
- Whipple KX, Wobus C, Crosby B, Kirby E, Sheehan D (2007) New tools for quantitative geomorphology: extraction and interpretation of stream profiles from digital elevation data. *GSA annual meeting*, 28 October 2007, special bulletin. Boulder, CO
- Wobus C, Crosby B, Whipple KX (2006) Hanging valleys in fluvial systems: control on occurrence and implications for landscape evolution. *J Geophys Res* 111:F02017